Microstructural characterization of the HAZ in AISI 444 ferritic stainless steel welds

Cleiton C. Silva[a,*], *Jesualdo P. Farias*[a], *Hélio C. Miranda*[a], *Rodrigo F. Guimarães*[a], *John W.A. Menezes*[b], *Moisés A.M. Neto*[c]

[a]*Federal University of Ceará, Department of Materials and Metallurgical Engineering, Welding Engineering Laboratory, Campus do Pici, Building 715, CEP 60455-760, Fortaleza, Ceará, Brazil*

[b]*Federal University of Ceará, Department of Materials and Metallurgical Engineering, Materials Characterization Laboratory, Campus do Pici, Building 720, CEP 60455-760, Fortaleza, Ceará, Brazil*

[c]*Federal University of Santa Catarina, Department of Mechanical Engineering, POLO-Laboratórios de Pesquisa em Refrigeração e Termofísica, Florianópolis, Santa Catarina, Brazil*

ARTICLE DATA

Article history:
Received 24 January 2007
Received in revised form 7 March 2007
Accepted 14 March 2007

Keywords:
Welding
HAZ
Microstructure
Secondary phases
AISI 444

ABSTRACT

Ferritic stainless steel is used as a coating for equipment in the petroleum refining industry. Welding is the main manufacturing and maintenance process used. However, little information on the metallurgical alterations caused by welding of these steels is found in the literature, prompting this study. In this study the authors evaluated the HAZ microstructure of AISI 444 ferritic stainless steel welded plates, by scanning electron microscopy (SEM) and X-ray diffraction (XRD). The results indicated that a weld thermal cycle caused microphase precipitation in the HAZ of the ferritic stainless steel. Also needle-like Laves phase precipitation occurred in the HAZ, near the partially-melted zone. Other secondary phases such as chi and sigma were observed, as well as nitride, carbide and carbonitride precipitates.

1. Introduction

Stainless steels can suffer various forms of metallurgical damage when exposed to critical temperatures. In welding, the region of the heat affected zone (HAZ) often experiences temperatures that are sufficient to promote microstructural changes. The formation of undesirable phases may cause a deleterious effect on the mechanical and corrosion resistance properties of the steels. Notably, amongst the main secondary phase precipitates which can occur during welding in stainless steel are carbides, nitrides and intermetallic compounds.

The precipitation of chromium nitrides, carbides and carbonitrides may occur under various conditions, depending on the stainless steel grade. During the welding of ferritic stainless steels, chromium carbides are formed in the HAZ region at locations that were heated to temperatures above 900 °C. In some cases, ferritic stainless steels regain their original resistance after tempering in the 650–800 °C range [1]. However, when these steels are produced with low interstitial elements like carbon and nitrogen, the precipitation is less likely to occur. According to the literature, all stainless steels with carbon content above 0.001% are susceptible to carbide precipitation [1,2]. Chromium carbide precipitation may be responsible for embrittlement, intergranular corrosion and may reduce resistance to pitting corrosion.

The precipitation of sigma (σ), chi (χ) and Laves phases in stainless steels can cause embrittlement and a decrease in

* *Corresponding author*. Universidade Federal do Ceará, Departamento de Engenharia Metalúrgica e de Materiais, Laboratório de Engenharia de Soldagem, Campus do Pici, Bloco 715, Fortaleza, Ceará, Brazil. Tel.: +55 85 33669358.
E-mail address: cleitonufc@yahoo.com.br (C.C. Silva)

1044-5803/$ – see front matter © 2007 Elsevier Inc. All rights reserved.
doi:10.1016/j.matchar.2007.03.011

Table 1 – Chemical composition of the AISI 444 ferritic stainless steel (wt.%)

C	Cr	Ni	Mo	Nb	Ti	N	Fe
0.015	17.55	0.20	1.85	0.16	0.13	0.012	Bal

corrosion-resistance [3,4]. The σ phase has a tetragonal crystal structure, formed mainly of iron and chromium but it may also contain molybdenum. Its formation field phase is defined in the Fe–Cr diagram at temperatures below 840 °C. However, variations in the chromium and molybdenum contents modify the kinetic reactions, moving the precipitation temperature to as high as 1000 °C [5]. In steels with low chromium content, the σ phase forms very slowly, and is unlikely to occur during a welding cycle. However, when the steel contains levels of chromium above 20%, σ phase precipitation is possible. Thus, during heat treatment and welding, the cooling rate must be high to avoid precipitation of this phase.

Molybdenum also promotes χ (chi) and Laves phase precipitation. The χ phase according to the literature has a $Fe_{36}Cr_{12}Mo_{10}$ nominal composition. Because of the high levels of chromium and molybdenum removed from the matrix by its precipitation, this phase causes a decrease in corrosion-resistance and increases embrittlement of the steel [5]. The Laves phase is an intermetallic compound that can occur in complex chemical compositions. Machado and Padilha [12] cite that some elements like molybdenum, titanium and niobium can favor Laves phase formation, and that the presence of silicon and niobium may promote $(Fe, Ni, Cr)_2(Nb, Si)$ Laves phase precipitation.

A frequent problem in many ferritic and duplex stainless steel is the 475 °C embrittlement, which causes a significant reduction of toughness and ductility at room temperature but causes a considerable increase in the strength and hardness [6–8]. The 475 °C embrittlement probably causes, in addition to alterations in mechanical properties, a decrease in corrosion-resistance owing to spinodal decomposition of ferrite in the Cr-rich α' phase [9,10].

All of these factors can cause damage to stainless steels during the welding process. Consequently, it is necessary to study the metallurgical changes occurring in the welding of these steels. This work presents observations made of the HAZ in AISI 444 ferritic stainless steel welded by the SMAW process.

2. Materials and Procedure

The material evaluated in this work was the AISI 444 ferritic stainless steel (FSS) base metal, whose chemical composition is shown in Table 1. The covered electrode used was AWS E 309MoL-16 austenitic stainless steel with a 2.5 mm diameter. The use of this covered electrode was suggested by PETROBRAS technicians. The chemical composition of the weld metal is presented in Table 2.

Table 2 – AWS E309MoL-16 austenitic stainless steel weld metal chemical composition (wt.%)

C	Cr	Ni	Mo	Fe
0.03	23	13	2.5	Bal

Table 3 – Welding parameters used for this study

RMS current (A)	RMS voltage (V)	Welding speed (cm/min)	Welding energy (kJ/cm)
80	25	20.0	6.0
80	25	12.5	9.0
80	26	10.0	12.0

The manual welding was carried out with a single deposition in the plane position on plates 50×150 mm in size and 3.0 mm thick, using the SMAW process. An INVERSAL 450 multiprocess power source system for data acquisition and a system to assist the welding speed control were used. Three levels of welding energy were employed with parameters: RMS current, RMS voltage, welding speed and energy are shown in Table 3.

The samples were prepared using routine metallographic methods and etching with Vilella's reagent (1 g picric acid, 100 ml ethanol, 5 ml hydrochloric acid). Microstructural characterization was carried out using an Olympus optical microscope with an image analysis system Image ProPlus and an XL Phillips® scanning electron microscope (SEM) equipped with an energy dispersive X-ray (EDX) system.

X-ray diffraction analysis (XRD) was carried out to qualitatively characterize the precipitate types in the HAZ of the samples welded. This analysis was carried out with an X'Pert Phillips® X-ray diffractometer, CuKα radiation (λ = 0.1542 nm) and a diffracted beam monochromator. Data acquisition was made using the software package belonging to the equipment (X'Pert Data Collector, X'Pert Graphs and Identify, X'Pert Organizer).

3. Results and Discussion

3.1. *Microstructural Analysis*

The AISI 444 FSS as-cast weld consisted of a single phase microstructure of polygonal ferrite with some titanium and niobium carbonitrides (Fig. 1). These carbonitrides occur

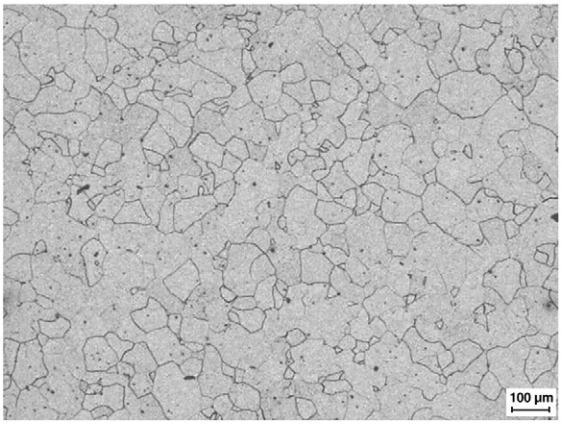

Fig. 1 – Microstructure of the base metal obtained by optical microscopy. Particles are titanium and niobium carbonitrides. Etching: Vilella's reagent.

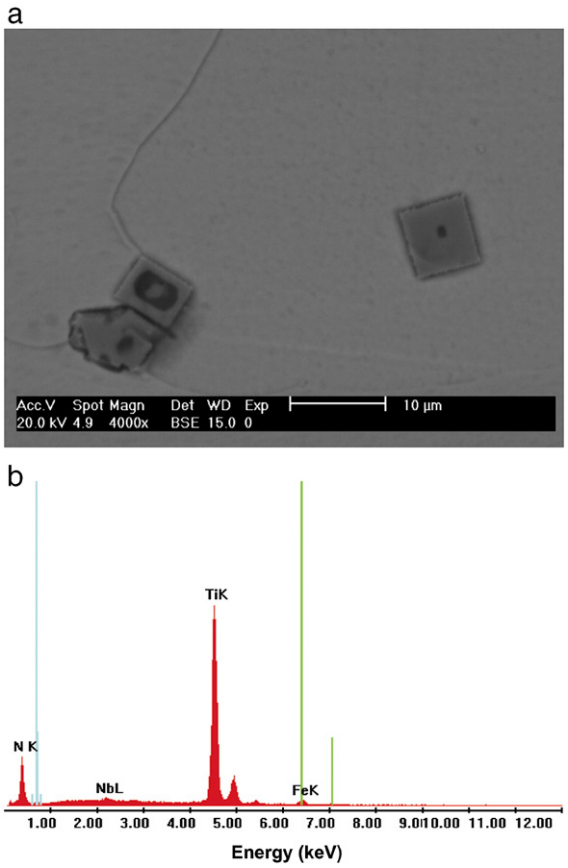

Fig. 2 – (a) Titanium and niobium carbonitride precipitates. (b) EDX analysis of the carbonitride precipitates.

because this steel contains titanium and niobium to stabilize carbon and nitrogen and avoid sensitization. Fig. 2a shows titanium and niobium carbonitrides in detail in the original microstructure of the base metal. The EDX analysis shows the presence of nitrogen, niobium and titanium peaks (Fig. 2b).

In the HAZ adjacent to the weld bead, the ferrite underwent considerable grain coarsening (Fig. 3) due to heating above 1100 °C in this region. The HAZ grain growth causes a decrease in toughness and consequently limits application in some

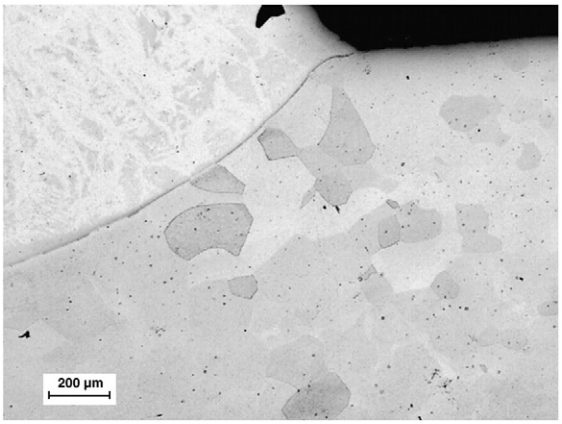

Fig. 3 – HAZ microstructure of AISI 444 steel welded with 6 kJ/cm. Etching: Vilella's reagent.

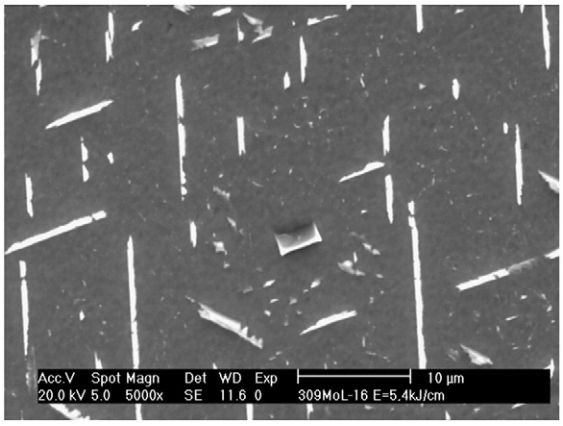

Fig. 4 – Detail of the needle-like precipitates in the HAZ. Etching: Vilella's reagent.

cases. Various very fine precipitates with a needle-like morphology were observed in the HAZ near the partially-melted zone, Fig. 4. Owing to their limited size, it was not possible to determine the chemical composition by EDX analysis.

Faria [11] studied the presence of these phases in the HAZ of ferritic stainless steels containing 17% and 18% chromium and additions of niobium and molybdenum. Using transmission electron microscopy (TEM), he determined the chemical composition of the particles, which were rich in niobium and molybdenum. This result suggested that the phase is probably a Laves phase. Machado and Padilha [12] also verified that elements like niobium, titanium and molybdenum contribute to promoting Laves phase formation and concluded that the presence of this phase in these steels caused a considerable decrease in toughness.

Three observations involving the microphases presented in AISI 444 FSS and the microphases observed in Faria's work [11] are worth noting. The first is that in both cases the region where the Laves phase precipitation was observed was in the HAZ near the partially-melted zone. The second observation is the needle-like morphology observed in all cases. The third observation is that the niobium content of the two steels is approximately equal (0.16% Nb). Based on these facts, it is probable that the phases present in the HAZ of the AISI 444 FSS examined here are Laves phases.

Although the niobium and titanium in the alloy are normally present in the form of carbonitrides, if the steel is heated to sufficiently high temperatures, the carbon and nitrogen can be redissolved and the niobium and titanium put back into solution, free to associate with elements such as iron and chromium, giving origin to the Laves phase. This is possible since the HAZ region where the Laves phases are observed is precisely at the temperature range in which carbides, nitrides and carbonitrides exhibit substantial solubility, above 1100 °C, according to the time-temperature precipitation (TTP) diagram, Fig. 5.

Several other researchers have presented results for Laves phase precipitation in ferritic and duplex steels [15–22]. Sakasegawa et al. [15], on studying the effect of precipitation morphology on ferritic/martensitic stainless steel toughness, verified that in materials aged at 650 °C, the M_6C disappeared and the Laves phase appeared. The authors also noted that the

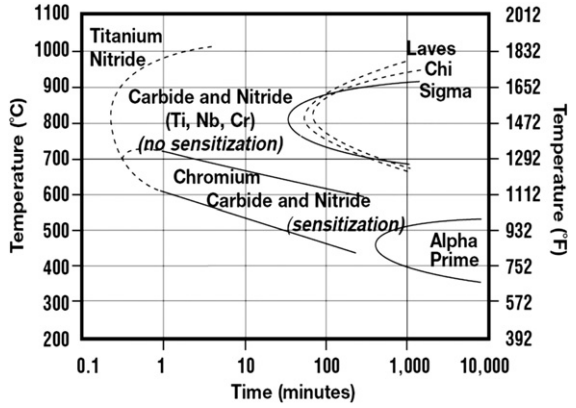

Fig. 5 – Isothermal precipitation diagram of secondary phases in ferritic stainless steels [13,14].

amount of precipitation increased up to 1000 h but that further change between 1000 and 3000 h was very small. However, in all cases the precipitation occurred over long time exposures. In welding, cooling rates are very rapid; however, it is possible that some non-equilibrium mechanism acts in the partially-melted zone, and is capable of promoting the formation of secondary phases such as Laves phase.

Therefore, below the temperature where the Laves phases formed, a fine network that formed along the ferrite grain boundaries was seen, as well as the presence of very fine intragranular precipitation, Fig. 6. It is believed that the grain boundary precipitation is the σ-phase and that the very small intragranular precipitates are the χ-phase. The σ-phase is an intermetallic Fe–Cr phase, with variable composition in high-alloy steels. In general, the nucleation of σ-phase occurs at the grain boundary, growing into the ferrite [23]. Several factors influence σ-phase formation, including the chemical composition. According to Sourmail [24], elements such as Cr, Mo, Nb and Ti are known to promote σ formation. Another important fact is that σ-phase formation in ferrite is about 100 times faster than in austenite [25]. AISI 444 is essentially ferritic with a composition that contains the main elements that promote the σ-phase. Moreover, it is probable

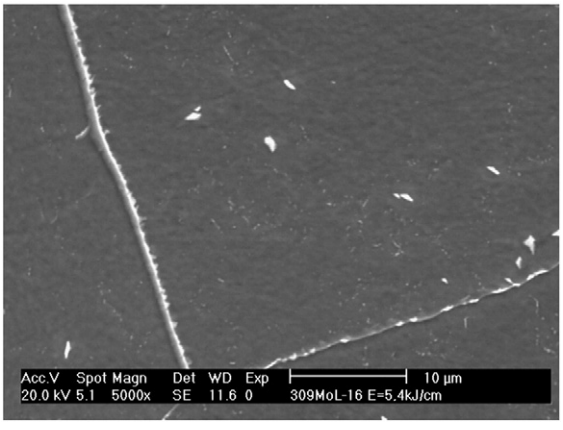

Fig. 6 – Fine inter- and intragranular precipitation at and near a ferrite grain boundary. The intergranular precipitates are probably σ-phase, whereas the intragranular precipitation is more likely χ-phase.

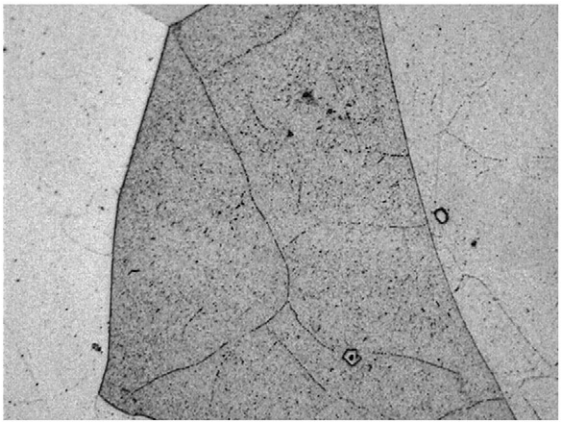

Fig. 7 – Precipitation in the HAZ of AISI 444 welded with 6 kJ/cm. Etching: Vilella's reagent.

that the σ-phase that forms along the ferrite grain boundaries is assisted by the presence of χ-phase, since this phase is considered a facilitator for σ-phase formation [26].

Another microstructural alteration observed in the HAZ of AISI 444 FSS was the presence of finely dispersed precipitates in both the matrix and in the ferrite grain boundaries, Fig. 7. In many

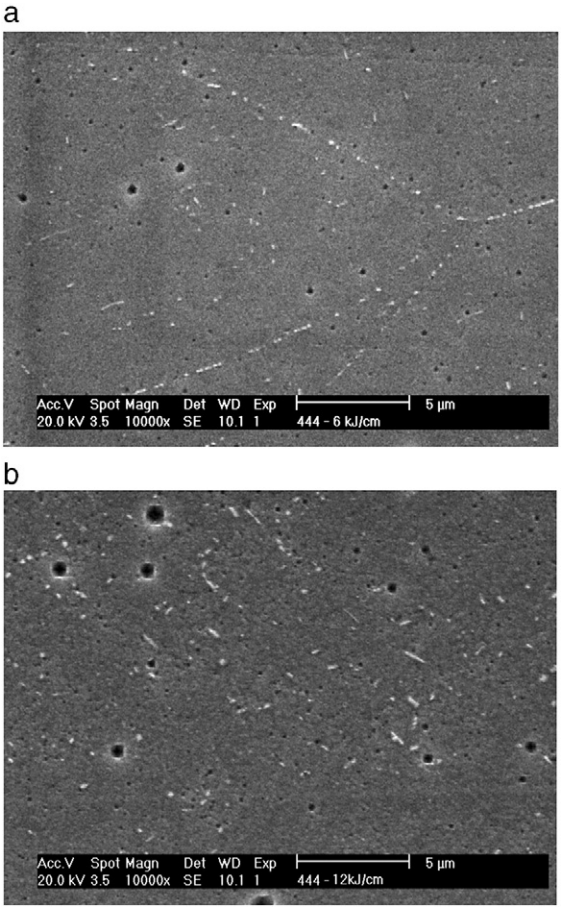

Fig. 8 – SEM images of precipitation in the HAZ at: (a) a sub-grain boundary, (b) the center of a grain. Sample welded with 6 kJ/cm. Etching: Vilella's reagent.

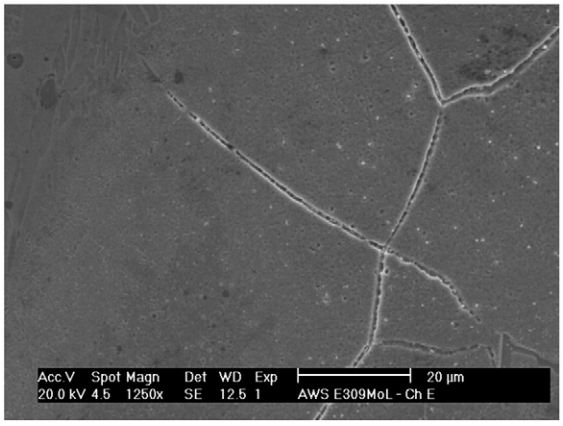

Fig. 9 – SEM image of precipitation at a ferrite grain boundary in a sample welded with 9 kJ/cm. Note the grain boundary ditching caused by removal of chromium carbide precipitates during metallographic polishing. Etching: Vilella's reagent.

cases, the presence of precipitates along the ferrite sub-grain boundaries can be seen. The structure shown in Fig. 7 is in the HAZ near the weld bead of a sample welded with 6 kJ/cm. In this region the temperatures reached were greater than 900 °C, which provides favorable conditions for possible chromium carbide and/or nitride precipitation. Liao [27] simulated the weld heating cycle in duplex stainless steel and verified the formation of CrN and Cr_2N in the ferrite, due to the high diffusivity of chromium and nitrogen and the low solubility of nitrogen in this phase.

Using SEM it was possible to observe the precipitates in the HAZ, as shown in Fig. 8. In Fig. 8(a), precipitation is observed at grain and sub-grain boundaries in the specimen welded with 6 kJ/cm. The size of the precipitates is quite small, making EDX analysis of the particles unfeasible. The large polygonal (dark) points in both Fig. 8(a) and (b) are believed to be titanium nitrides. Fig. 8(b) shows the presence of precipitation inside a HAZ ferrite grain of the sample welded with 12 kJ/cm.

Fig. 9 presents an area in the HAZ of a sample welded with 9 kJ/cm where ditch formation in the grain boundary may be observed. The occurrence of ditches is characteristic of regions where chromium carbide precipitation has been pulled out in the metallographic polishing operation.

3.2. *X-ray Diffraction Analysis*

A qualitative analysis of the precipitate carried out by X-ray diffraction was based on the identification of the peaks after refinement, using PROFIT and PCPDFWIN software to adjust the exact peak angular position of the phases presented in the HAZ. Based on the values of the peaks in the diffractograms, a comparison with JCPDS card values was made, in order to identify the phases which could precipitate in the AISI 444 steel. Fig. 10 shows diffractograms of the samples welded with 6 and 12 kJ/cm. The presence of peaks corresponding to ferrite (α) and peaks of smaller intensity, which correspond to the precipitates, may be seen. The presence of several peaks inside a larger peak, using PROFIT software, was also noted.

The XRD results indicated the probable presence of several secondary phases such as χ, σ and Laves, besides carbides and

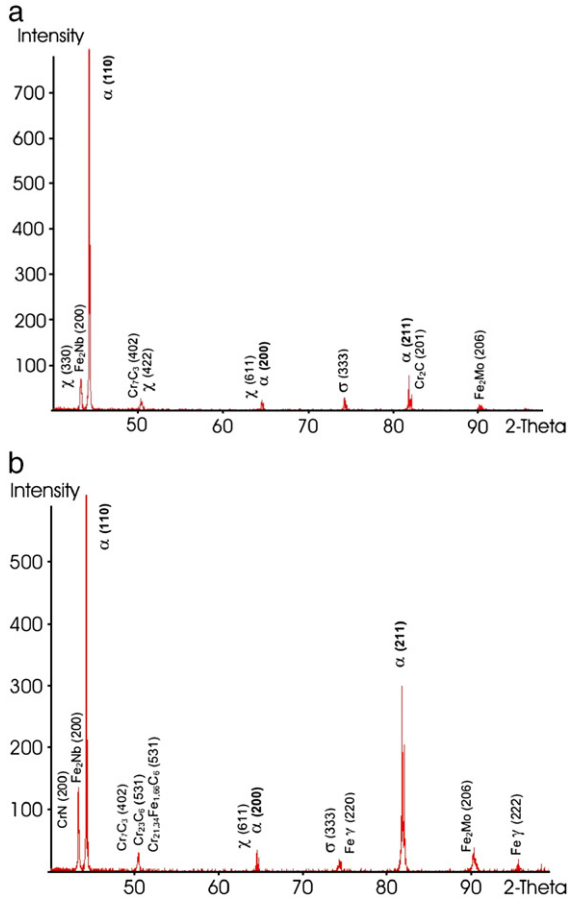

Fig. 10 – X-ray diffractograms showing ferrite and precipitate peaks. (a) a sample welded with 6 kJ/cm. (b) A sample welded with 12 kJ/cm.

nitrides. Fig. 10 indicates the probable presence of small amounts of Laves phases, identified as Fe_2Nb and Fe_2Mo. Another phase probably present in all analyses was the χ-phase; this phase was seen in three peaks in the X-ray diffractogram of the sample welded with 6 kJ/cm, Fig. 10(a), and at one peak for a sample welded with 12 kJ/cm, Fig. 10(b). The probable presence of σ-phase was also observed (Table 4).

Table 4 – Secondary phase precipitation identified by XRD

Precipitates	Peak locations (2θ)/associated planes — for different welding energies		
	6 kJ/cm	9 kJ/cm	12 kJ/cm
Laves (Fe_2Nb)	43.39°/(200)	43.37°/(200)	43.39°/(200)
χ	50.41°/(330) 64.59°/(422) 64.73°/(611)	64.57°/(611)	64.71°/(611)
σ	74.23°/(333)	74.43°/(333)	74.37°/(333)
CrN	–	43.69°/(200)	43.69°/(200)
Cr_2C	~82°/(201)	–	–
Cr_7C_3	50.39°/(402)	–	–
$Cr_{23}C_6$	–	50.69°/(531)	50.69°/(531)
$Cr_{21.34}Fe_{1.66}C_6$	–	–	50.69°/(531)
Cr_7C_3	–	50.49°/(402)	50.51°/(402)
Laves (Fe_2Mo)	90.12°/(206)	90.11°/(206)	90.12°/(206)

Through the diffractograms it was possible to verify that, for the sample welded with low heat input (6 kJ/cm), the carbides present were of the Cr_2C and Cr_7C_3 types. However, for the sample with a larger heat input (12 kJ/cm) these precipitates were not observed, but more complex carbides such as $Cr_{23}C_6$, $Cr_{21.34}Fe_{1.66}C_6$ and Cr_7C_3, as shown in Fig. 10(b).

4. Conclusions

Based on the experimental results obtained for the welding conditions used in this work, it was possible to conclude that the HAZ of the AISI 444 stainless steel welded with the AWS E309MoL-16 covered electrode exhibited significant grain growth with respect to the base metal in the partially-melted zone.

The presence of fine needle-like precipitation close to the partially-melted zone was observed; this was judged to be Laves phase, based on similar research in the literature, and was present irrespective of the welding energy employed. The weld thermal cycle also caused finely dispersed precipitation in the HAZ. In some areas, the presence of chi and sigma phase precipitation was detected at the ferrite grain boundaries; these were particularly prominent in the samples welded with low energy.

The X-ray diffraction analyses confirmed the presence of secondary phases such as Laves, chi and sigma, in addition to the presence of several chromium nitrides and carbonitrides, reinforcing the observations of these phases obtained by microscopy, and consistent with the published literature.

Acknowledgments

The authors are grateful to ENGESOLDA and LACAM laboratories, to ACESITA for supplying the steel, to PETROBRAS for their collaboration and also to the Brazilian research agencies (CNPq, FINEP e ANP/PRH-31) for financial support.

REFERENCES

[1] Folkhard E. Welding metallurgy of stainless steels. New York: Spring-Verlag Wien; 1988.
[2] Kou S. Welding metallurgy. New York: John Wiley & Sons; 1987.
[3] Ravindranath K, Malhotra SN. The influence of aging on the intergranular corrosion of 22 chromium-5 nickel duplex stainless steel. Corros Sci 1995;37:121–32.
[4] Kim JS, Kwon H-S. Effects of Tungsten on corrosion and kinetics of sigma phase formation of 25% chromium duplex stainless steels. Corrosion 1999;55:512–21.
[5] ASM. ASM specialty handbook of stainless steels. ASM International; 1996.
[6] Van Zwieten ACTM, Bulloch JH. Some considerations on the toughness properties of ferritic stainless steels—a brief review. Int J Press Vessels Piping 1993;56:1–31.
[7] Tavares SSM, de Noronha RF, da Silva MR, Neto JM, Pairis S. 475 °C embrittlement in a duplex stainless steel UNS S31803. Mater Res 2001;4:237–40.
[8] Cortie MB, Pollak H. Embrittlement and aging at 475 °C in an experimental ferritic stainless steel containing 38 wt.% chromium. Mater Sci Eng A Struct Mater Prop Microstruct Process 1995;199:153–63.
[9] Grobner PJ. The 885 °F (475 °C) embrittlement of ferritic stainless steels. Metall Trans A Phys Metall Mater Sci 1973;4:251–60.
[10] Souza, J. A. Avaliação da Fragilização à 400 e 475°C do Aço Inoxidável Ferrítico AISI 444 Utilizado em Torres de Destilação de Petróleo. M.Sc. Thesis, Universidade Federal do Ceará, Ceará, Brazil; 2004. [in Portuguese]
[11] Faria, R. A. Efeito da composição química de aços inoxidáveis ferríticos no desempenho de juntas soldadas pelo processo a arco metálico gasoso (SAMG). M.Sc. Thesis, Universidade de São Paulo, São Paulo, Brazil; 2000. [in Portuguese]
[12] Machado IF, Padilha AF. The occurrence of Laves phase in Fe-15% Cr-15% Ni austenitic stainless steel containing niobium. Acta Microsc 2003;12:111–4.
[13] Brown EL. Intermetallic phase formation in 25Cr-3Mo-4Ni ferritic stainless steel. Metall Trans A Phys Metall Mater Sci 1983;14A:791.
[14] Nichol TJ, Datta A, Aggen G. Embrittlement of ferritic stainless steels. Metall Trans A Phys Metall Mater Sci 1980;11A:573.
[15] Korcakova L, Hald J, Somers MAJ. Quantification of Laves phase particles size in 9CrW steel. Mater Charact 2001;47:111–7.
[16] Kim SB, Paik KW, Kim YG. Effect of Mo substitution by W on high temperature embrittlement characteristics in duplex stainless steels. Mater Sci Eng A Struct Mater Prop Microstruct Process 1998;247A:67–74.
[17] Yamamoto K, Kimura Y, Wei FG, Michima Y. Design of Laves phase strengthened ferritic heat resisting steels in the Fe–Cr–Nb(–Ni) system. Mater Sci Eng A Struct Mater Prop Microstruct Process 2002;329–331:249–54.
[18] Dimmler G, Weinert P, Kozeschnik E, Cerjak H. Quantification of the Laves phase in advanced 9–12% Cr steels using a standard SEM. Mater Charact 2003;51:341–52.
[19] Park CJ, Ahn MK, Kwon HS. Influences of Mo substitution by W on the precipitation kinetics of secondary phases and the associated localized corrosion and embrittlement in 29% Cr ferritic stainless steels. Mater Sci Eng A Struct Mater Prop Microstruct Process 2006;418:211–7.
[20] Zucato I, Moreira MC, Machado IF, Lebrão SMG. Microstructural characterization and the effect of phase transformation on toughness of the UNS S31803 duplex stainless steel aged treated at 850 °C. Mater Res 2002;5:385–9.
[21] Miyahara K, Hwang JH, Shimoide Y. Aging phenomena before the precipitation of the bulky Laves phase in Fe–10% Cr ferritic alloys. Scr Metall Mater 1995;32:1917–21.
[22] Sakasegawa H, Hirose T, Kohyama A, Katoh Y, Harada T, Asakura K, et al. Effects of precipitation morphology on toughness of reduced activation ferritic/martensitic steels. J Nucl Mater 2002;307–311:490–4.
[23] Atamert S, King JE. Sigma-phase formation and its prevention in duplex stainless steels. J Mater Sci Lett 1993;12:1144–7.
[24] Sourmail T. Precipitation in creep austenitic stainless steels. Mater Sci Technol 2001;17:1–13.
[25] Barcik J. Mechanism of σ-phase precipitation in Cr–Ni austenitic steels. Mater Sci Technol 1988;4:5–15.
[26] Nilsson JO. The physical metallurgy of duplex stainless steel. Conference of duplex stainless steel 97. Proceedings; 1997. p. 43–71. The Netherlands.
[27] Liao J. Nitride precipitation in weld HAZs of a duplex stainless steel. ISIJ Int 2001;41:460–7.